



Superconducting State in a Gallium-Doped Germanium Layer at Low Temperatures

T. Herrmannsdörfer, V. Heera, O. Ignatchik, M. Uhlarz, A. Mücklich, M. Posselt, H. Reuther, B. Schmidt, K.-H. Heinig, W. Skorupa, M. Voelskow, C. Wündisch, R. Skrotzki, M. Helm, and J. Wosnitzer

Dresden High Magnetic Field Laboratory (HLD) and Institute of Ion Beam Physics and Materials Research, Forschungszentrum Dresden-Rossendorf (FZD), P.O. Box 51 01 19, D-01314 Dresden, Germany

(Received 29 January 2009; published 27 May 2009)

We demonstrate that the third elemental group-IV semiconductor, germanium, exhibits superconductivity at ambient pressure. Using advanced doping and annealing techniques of state-of-the-art semiconductor processing, we have fabricated a highly Ga-doped Ge (Ge:Ga) layer in near-intrinsic Ge. Depending on the detailed annealing conditions, we demonstrate that superconductivity can be generated and tailored in the doped semiconducting Ge host at temperatures as high as 0.5 K. Critical-field measurements reveal the quasi-two-dimensional character of superconductivity in the ~ 60 nm thick Ge:Ga layer. The Cooper-pair density in Ge:Ga appears to be exceptionally low.

DOI: 10.1103/PhysRevLett.102.217003

PACS numbers: 74.10.+v, 74.78.-w

Since the first observation of superconductivity in 1911, the search for new superconducting materials has offered quite a few surprises, such as the discovery of several classes of high- T_c compounds [1], but recently also the observation of superconductivity in the doped elemental semiconductors diamond [2] and silicon [3]. Although superconductivity has been observed in several doped binary semiconductors already starting in the 1960s, e.g., in doped tellurides such as GeTe [4], in SrTiO₃ [5], flanked and motivated by a considerable amount of theoretical work [6], as well as in SiC [7] recently, it has not been seen in the simple elemental representatives at ambient-pressure conditions before. Superconductivity of Si and Ge in their metallic high-pressure phases has been reported by Wittig already in 1966 [8]. However, it needed more than four decades to drive Si and diamond superconducting at ambient-pressure conditions, owed to the sophisticated preparation techniques required and maybe due to the prejudice that superconductivity might not be possible in the archetypical semiconductors. Compared to Si and diamond, Ge seems to be even less promising for the search of superconductivity as theoretical studies predict only a weak tendency towards superconductivity in heavily n -type [9] and p -type doped Ge [10].

In order to obtain superconductivity in group-IV semiconductors, heavy p -type doping well above the metal-insulator transition is required. Otherwise the charge-carrier density of these materials is too low to create a superconducting state at low temperatures. Ekimov *et al.* have observed superconductivity in diamonds containing high boron (B) concentrations prepared by a high-pressure and high-temperature technique at temperatures up to $T_c = 2.3$ K [2]. Bustarret *et al.* [3] have investigated boron-supersaturated Si layers processed by ultra-short-time laser melting and found superconductivity at $T_c = 0.34$ K. For this work, Ga has been chosen as acceptor atom due to its high solid solubility in Ge (up to ~ 1 at. % at 700 °C). Ion implantation as an effective method for introducing high

concentrations of dopants has been used. The ion-beam technique is highly selective since it allows for a precise control of the amount of the implanted species and its depth distribution. Here, we have succeeded in producing samples with a peak concentration of 8 at. % Ga in a thin layer of Ge with a full width at half maximum of approximately 60 nm (see Fig. 1). However, high-dose ion implantation causes severe lattice damage which may be difficult to anneal as observed for B-doped diamond where the formation of graphite may further complicate a reconstruction of the lattice [11,12] and where the superconducting phase might be located in amorphous boron-rich intergranular layers and pockets [13]. In Ge (and Si), annealing of implantation damage is easier to achieve than in diamond. Here, the challenge is to reconstruct the crystalline structure without causing long-range diffusion, precipitation, and subsequent clustering of acceptor atoms in the supersaturated semiconductor. Flashlamp annealing in the millisecond range is known to be a versatile tool to remove the implantation damage and to achieve dopant activation in thin semiconductor layers [14–16]. Because of the short thermal-processing time, this method is much less affected by diffusion and precipitation problems. Depending on light-pulse energy and duration, flashlamp annealing leads to solid-phase epitaxial or liquid-phase epitaxial regrowth of the amorphous layers formed during the high-dose implantation. Here, we have treated samples using various flashlamp fluences Φ after implanting. This resulted in samples with a slightly decreased peak concentration of 6 at. % Ga after annealing (see Fig. 1), corresponding to 2.6×10^{21} Ga atoms/cm³. No evidence for the formation of Ga clusters or filaments has been found during careful sample analysis. The charge-carrier concentration of the Ge:Ga samples has been determined at low temperatures, $T \leq 2.5$ K, by means of Hall-effect measurements (see inset of Fig. 3). A summary of the most important parameters of five samples is given in Table I. The hole concentration extracted from Hall measurements

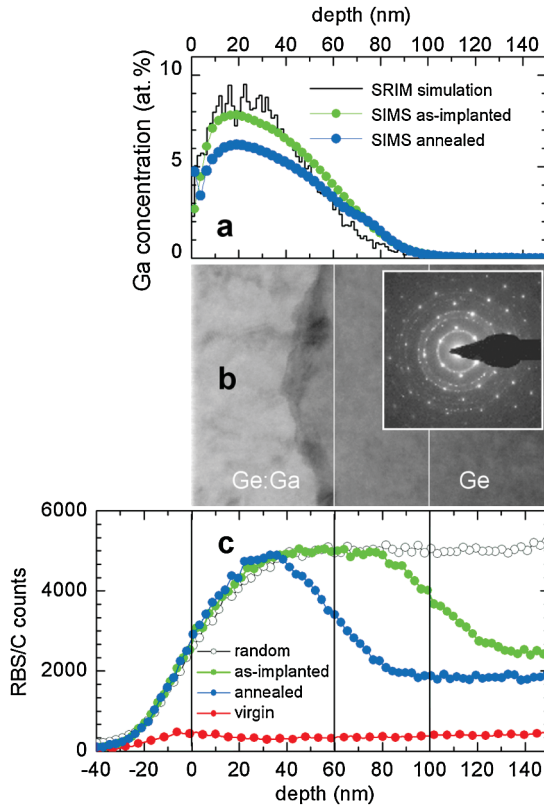


FIG. 1 (color). (a) Ga depth distribution obtained by secondary ion mass spectrometry (SIMS) of a Ge:Ga sample before and after annealing ($\Phi = 50.8 \text{ J/cm}^2$) compared to a Ga profile simulated for an as-implanted Ge:Ga sample using the SRIM code [22]. (b) The cross-sectional transmission electron micrograph and the diffraction pattern (inset) from the same region demonstrate that the implanted layer is completely (poly)recrystallized after flashlamp annealing down to about 50–60 nm, followed by $\approx 10 \text{ nm}$ thin wavy interface (indicated by the left white line) between the polycrystalline layer and the single-crystalline region. The initial amorphous-crystalline interface is indicated by the right white line. (c) Results of a channeled-ion Rutherford backscattering (RBS/C) analysis confirm the random orientation of the Ge grains. The backscattering signal for the annealed sample reaches the same value as in random orientation. For comparison the RBS/C results of unimplanted (virgin) and as-implanted Ge are shown.

varies considerably with the flashlamp fluence. At a small fluence, $\Phi = 45.5 \text{ J/cm}^2$, the hole concentration is up to 1 order of magnitude smaller than the Ga concentration determined from secondary ion mass spectrometry (SIMS), indicating the only partial electrical activation of the dopants. With increasing fluence, the hole concentration also increases to $1.4 \times 10^{21} \text{ cm}^{-3}$ reflecting that half of the implanted Ga atoms have been activated.

Measurements of the electrical-transport properties were carried out from 300 K to 20 mK and are presented in Fig. 2. Data were taken using low ac-excitation currents (down to 10 nA) in order to keep the electrical current density in the thin Ge:Ga layer moderate. The unimplanted sample exhibits the typical behavior of semiconducting

TABLE I. Fluence Φ used during 3 ms of flashlamp annealing, critical superconducting transition temperature T_c (taking the 50% drop of R), critical magnetic field aligned in plane, $B_{c\parallel}$, and perpendicular to the Ge:Ga layer, $B_{c\perp}$, as well as charge-carrier concentration obtained from Hall-effect measurement, n_{Hall} , of five Ge:Ga samples.

| Ge:Ga sample | a | b | c | d | e |
|--|------|-------------------|------|-------|------|
| $\Phi \text{ (J/cm}^2\text{)}$ | 45.5 | 48.1 | 50.8 | 53.6 | 62.4 |
| $T_c \text{ (K)}$ | ... | 0.14 ^a | 0.45 | 0.19 | ... |
| $B_{c\parallel} \text{ (T)}$ | ... | ... | 1.1 | 0.18 | ... |
| $B_{c\perp} \text{ (T)}$ | ... | ... | 0.30 | 0.025 | ... |
| $n_{\text{Hall}} \text{ (10}^{21} \text{ cm}^{-3}\text{)}$ | 0.28 | 0.32 | 0.43 | 1.4 | 1.0 |

^aFor sample b, a nonzero residual resistance was measured at $T < T_c^*$.

bulk n -type Ge with a resistance drop due to the increasing mobility upon lowering the temperature, and a subsequent resistance increase due to carrier freeze-out. The as-implanted Ge:Ga sample also shows an increasing resistance below about 40 K despite the high doping level. This is due to the large damage induced by implantation and implies that the dopants are not electrically activated. In contrast, the sample which has been flashlamp annealed (fluence $\Phi = 53.6 \text{ J/cm}^2$) for $t = 3 \text{ ms}$ exhibits metallic behavior, indicating that a significant part of the dopants has been electrically activated. Below $T = 0.5 \text{ K}$, the resistivity drops to zero (Fig. 2) indicating the onset of superconductivity. In more detail, in the inset of Fig. 2 it is shown how the annealing conditions influence the normal and superconducting properties of the Ge:Ga samples. The residual normal-state resistivity is clearly affected by the annealing conditions. Upon increasing flashlamp fluence, the residual resistivity drops by a factor of 3. Compared to that, we observed a more elaborate dependence of the superconducting properties on the annealing conditions (see Table I). By keeping the flashlamp expo-

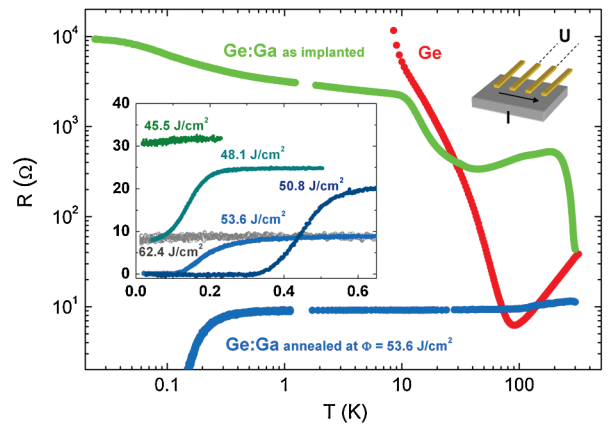


FIG. 2 (color). Temperature dependence of the electrical resistance of unimplanted Ge and as-implanted as well as annealed Ge:Ga ($\Phi = 53.6 \text{ J/cm}^2$, $t = 3 \text{ ms}$) taken in $B = 0$. Only annealed Ge:Ga exhibits superconductivity below 0.5 K, depending on the flashlamp fluence Φ (see inset).

sure time constant (3 ms) but varying the fluence stepwise in the range $45 \leq \Phi \leq 62.4 \text{ J/cm}^2$, and consequently varying the maximum annealing temperature, the occurrence of superconductivity can be triggered and, when further increasing Φ , even suppressed. The fluence of 45.5 J/cm^2 is not yet sufficient to induce a sample modification which allows for the creation of a superconducting state. At $\Phi = 48.1 \text{ J/cm}^2$, the onset of superconductivity is visible (inset of Fig. 2) and the highest transition temperature, $T_c = 0.45 \text{ K}$, is achieved at $\Phi = 50.8 \text{ J/cm}^2$. Tuning the annealing conditions to higher fluences, superconductivity starts to disappear. At $\Phi = 53.6 \text{ J/cm}^2$, T_c is reduced to about 0.2 K and at $\Phi = 62.4 \text{ J/cm}^2$ a superconducting transition has not been observed in the temperature range accessible to us, i.e., at $T \geq 20 \text{ mK}$. The reproducibility of the annealing process with respect to the creation of superconductivity has been verified for several samples prepared separately under identical conditions. Thus superconductivity only occurs in a narrow region of optimized parameters; in particular, the activation of charge carriers appears to be rather delicate. It should be mentioned that the maximum T_c is not observed in the sample with the largest charge-carrier concentration $1.4 \times 10^{21} \text{ cm}^{-3}$, but in the sample that has only one third, $0.43 \times 10^{21} \text{ cm}^{-3}$, of the highest level of activated Ga atoms instead. The width of the superconducting transition is rather broad, reflecting the inhomogeneous charge-carrier profile of the Ge:Ga layers.

The superconducting transition temperature of Ge:Ga, $T_c \leq 0.45 \text{ K}$, compares well to the one of B-doped diamond [2], C:B, taking into account the qualitative expectation of phonon-mediated superconductors, $T_c \sim \Theta_D$. Whereas the ratios of the superconducting transition temperatures, $T_c(\text{C:B})/T_c(\text{Ge:Ga}) = 5.1$, and of the Debye temperatures, $\theta_D(\text{C:B})/\theta_D(\text{Ge:Ga}) = 1860 \text{ K}/374 \text{ K} = 5.0$, match well, the comparison of these properties with the data of B-doped Si [3] ($T_c = 0.34$, $\Theta_D = 645 \text{ K}$) is less striking and might emphasize the influence of doping levels and individual electron-phonon coupling on the superconducting state of group-IV semiconductors. However, a reasonable scaling of T_c and Θ_D might support the notion of phonon-mediated superconductivity in this material class. Although the critical temperature of Ge:Ga is about 0.5 K , the critical magnetic field, B_c , reaches a value slightly above 1 T (see Table I). Both samples that undergo a complete superconducting transition exhibit a distinct dependence of the superconducting critical field on its orientation relative to the Ge:Ga layer. Superconductivity remains stable to clearly higher critical magnetic fields, $B_{c\parallel}$, when aligned in plane compared to when aligned perpendicular to the Ge:Ga plane, $B_{c\perp}$. The anisotropy reaches a maximum in the sample which has been annealed at $\Phi = 53.6 \text{ J/cm}^2$ where $B_{c\parallel}/B_{c\perp} = 7$ (see Fig. 3). From a qualitative point of view, this strong anisotropy of the critical magnetic field is typical for a thin-layered superconductor and may be considered as proof

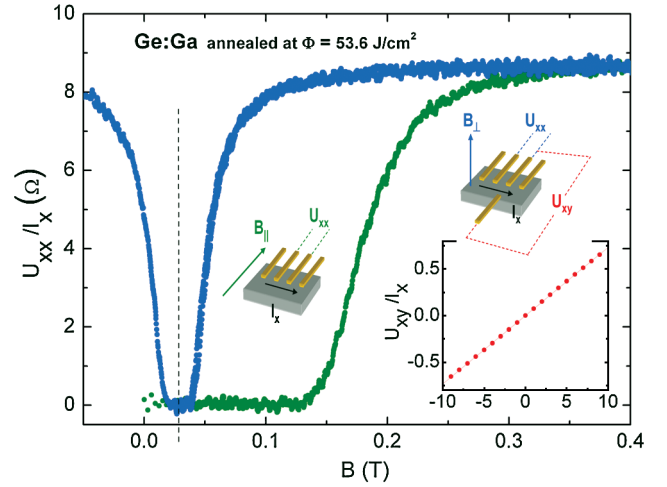


FIG. 3 (color). Electrical-transport data of a Ge:Ga sample (flashlamp annealed at $\Phi = 53.6 \text{ J/cm}^2$) as function of the magnetic field aligned in plane B_{\parallel} (green), and perpendicular B_{\perp} (blue). The offset of B (dashed line at $\sim 27 \text{ mT}$) results from frozen flux in the superconducting 20 T magnet after Hall-effect measurements (red data in inset).

that Ga is incorporated in the Ge matrix homogeneously in a thin layer in agreement with our structural analysis. The anisotropy of the superconducting critical field also allows for excluding superconductivity mediated by Ga clusters in the samples. The maximum possible in-plane fields, $B_{c\parallel}$, are attributed to the so-called Pauli limit where the high polarization of the electron spins is responsible for Cooper-pair breaking, whereas $B_{c\perp}$ is considered to be related to the orbital-limiting fields. It is remarkable that the theoretical Pauli limit in simple approximation [17], $B_P/T_c = 1.84 \text{ (T/K)}$, is exceeded in the sample with the highest T_c (0.45 K) and $B_{c\parallel}$ ($\sim 1.1 \text{ T}$) annealed at 50.8 J/cm^2 , where $B_{\parallel}/T_c = 2.4 \text{ (T/K)}$ (see Fig. 4). However, the large relative width of the superconducting transition hinders further conclusions. The temperature dependences of $B_{c\parallel}(T)$ and $B_{c\perp}(T)$ clearly deviate from the one of a simple bulk BCS superconductor, $B_c(T) = B_{c0}[1 - (T/T_{c0})^2]$. Even the Werthamer-Helfand-Hohenberg (WHH) theory [18] as a quantitative approach for type-II superconductors with a linear upper critical field, $B_{c2}(T) \sim T$ at $T > 0.5T_{c0}$, does not reasonably describe the critical field of Ge:Ga as $B_{c\parallel}(T)$ is linear down to lower temperatures, $0.1T_{c0}$, and $B_{c\perp}(T)$ is even superlinear at $T < T_{c0}$. A more detailed study of the curvature of $B_{c\parallel,\perp}(T)$ will be the subject of a more extended work on Ge:Ga where various scenarios for deviations from WHH theory (see, e.g., Boebinger *et al.* [19]) will be taken into account. From the orbital-limiting critical field, we deduce the coherence length as in the case of bulk superconductors according to $\xi = (\phi_0/2\pi B_{c\perp})^{1/2}$, where $\phi_0 = h/2e = 2.068 \times 10^{-15} \text{ Wb}$ is the flux quantum. From $B_{c\perp}$, one obtains $\xi = 33 \text{ (115) nm}$ for $\Phi = 50.8 \text{ (53.6) J/cm}^2$. These values may be taken to estimate the in-plane critical field, $B_{c\parallel}(\xi) = \sqrt{6}\phi_0/(\pi\xi d)$, where d

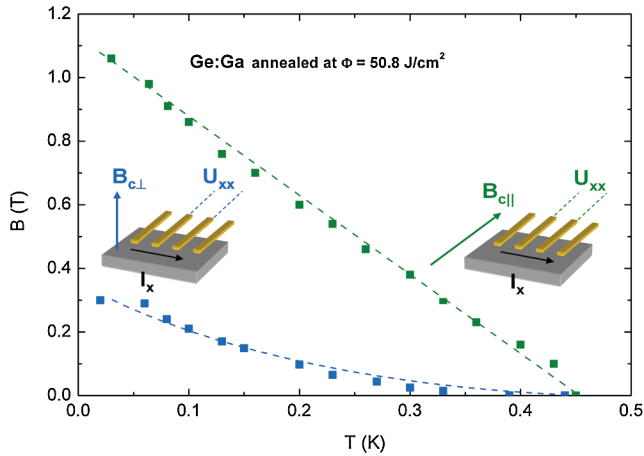


FIG. 4 (color). Field-temperature phase diagram of the Ge:Ga sample (flash lamp annealed at $\Phi = 50.8 \text{ J/cm}^2$) with the highest T_c at 0.45 K for two magnetic-field orientations relative to the Ge:Ga plane (see illustrations).

is the thickness of the Ga-doped layer and $\sqrt{6}$ is a correction factor for a thin-plate geometry [20]. Using $d = 60 \text{ nm}$ leads to $B_{c\parallel}(\xi) = 0.81 \text{ (0.23) T}$ for $\Phi = 50.8 \text{ (53.6) J/cm}^2$, in reasonable agreement with the experimental values (Table I). By use of the nonlinear Ginzburg-Landau theory, the critical-current density J_c of a thin-film superconductor may be estimated [21] using $J_c = ehn_s/(3\pi\sqrt{3}m\xi)$. We have measured a critical superconducting current of about $10 \mu\text{A}$. Using the superconducting critical-current density, $J_c = 10 \mu\text{A}/(1 \text{ cm} \times 60 \text{ nm}) = 1.7 \times 10^4 \text{ A/m}^2$ (spanned by the 60 nm thick Ga-doped Ge layer and the sample width of 1 cm) and the above calculated coherence length ξ , allows for an estimate of n_s . We obtain a superconducting charge-carrier density, $n_s = 2.7 \times 10^{14} \text{ cm}^{-3}$ ($\Phi = 53.6 \text{ J/cm}^2$), which is by orders of magnitude smaller than the normal-conducting charge-carrier density, deduced from Hall measurements, $n \approx 1 \times 10^{21} \text{ cm}^{-3}$. In this context, an effective mass of the charge carriers equal to the bare mass of free electrons, $m = m_e$, has been used for simplicity. In the case of light holes, $m \ll m_e$, n_s would be even smaller. Using $\lambda_L = \sqrt{m/(\mu_0 n_s e^2)}$ for the calculation of the London penetration depth leads to λ_L of the order of $10^2 \mu\text{m}$. Such a large London penetration depth makes the detection of superconductivity by inductive measurements virtually impossible in our thin Ge:Ga layers. Also the observation of a superconducting transition of Ge:Ga by means of heat capacity and NMR will be challenging as only a tiny jump of specific heat and an exiguous decrease of Pauli susceptibility and NMR Knight shift can be expected due to the very low Cooper-pair density. Therefore, the transport measurements reported here appear to be the only reliable means for the proof of superconductivity. According to λ_L/ξ of about $10^3\text{--}10^4$, Ge:Ga may be

considered as a superconductor in the extreme type-II limit.

In summary, the finding of superconductivity in Ga-doped Ge layers sheds new light on doped elemental semiconductors which might even serve as superconducting model systems as they allow for a tuning of their superconducting parameters via a modification of their hole concentration. The combination of ion implantation and subsequent flashlamp annealing can be employed to fabricate tailored thin-layer superconductors. Although the critical superconducting temperatures of Ge:Ga are far below those of high-temperature superconductors, there is a qualitative relationship between these systems concerning their $T_c(x)$ -phase diagrams. Both in the high-temperature superconductors and in Ge:Ga, there is a limited range of the charge-carrier (hole) concentration x which allows for the occurrence of superconductivity, and there is an optimum concentration where $T_c(x)$ is maximum. For further conclusions, of course, it would be of interest to explore the detailed relation between annealing parameters, carrier density, as well as critical temperatures and to also try other dopants in order to generate superconductivity in Ge.

The authors acknowledge the support of F. Arnold, M. Bartkowiak, and R. Beyer (FZD) for transport measurements as well as of H. Hortenbach and S. Teichert (Qimonda Dresden) for SIMS analysis. Part of this work was supported by EuroMagNET.

- [1] J. Bednorz and K. A. Müller, *Z. Phys. B* **64**, 189 (1986).
- [2] E. A. Ekimov *et al.*, *Nature (London)* **428**, 542 (2004).
- [3] E. Bustarret *et al.*, *Nature (London)* **444**, 465 (2006).
- [4] R. A. Hein *et al.*, *Phys. Rev. Lett.* **12**, 320 (1964).
- [5] J. F. Schooley *et al.*, *Phys. Rev. Lett.* **12**, 474 (1964).
- [6] C. S. Koonce *et al.*, *Phys. Rev.* **177**, 707 (1969).
- [7] Z. Ren *et al.*, *J. Phys. Soc. Jpn.* **76**, 103710 (2007).
- [8] J. Wittig, *Z. Phys.* **195**, 215 (1966).
- [9] W. Klose, *Adv. Solid State Phys.* **7**, 1 (1967).
- [10] L. Boeri *et al.*, *Phys. Rev. Lett.* **93**, 237002 (2004).
- [11] T. Tshepe, *et al.*, *Phys. Rev. B* **70**, 245107 (2004).
- [12] V. Heera *et al.*, *Diam. Relat. Mater.* **17**, 383 (2008).
- [13] N. Dubrovinskaia *et al.*, *Proc. Natl. Acad. Sci. U.S.A.* **105**, 11 619 (2008).
- [14] W. Skorupa *et al.*, *J. Electrochem. Soc.* **152**, G436 (2005).
- [15] M. Voelskow *et al.*, *Appl. Phys. Lett.* **87**, 241901 (2005).
- [16] R. A. McMahon *et al.*, *Vacuum* **81**, 1301 (2007).
- [17] A. M. Clogston, *Phys. Rev. Lett.* **9**, 266 (1962).
- [18] E. Helfand *et al.*, *Phys. Rev. Lett.* **13**, 686 (1964); *Phys. Rev.* **147**, 288 (1966); N. R. Werthamer *et al.*, *Phys. Rev.* **147**, 295 (1966).
- [19] G. Boebinger *et al.*, *Phys. Rev. B* **46**, 5876 (1992).
- [20] M. Tinkham, *Phys. Rev.* **129**, 2413 (1963).
- [21] L.-P. Levy, *Magnetism and Superconductivity* (Springer, New York, 2000).
- [22] J. F. Ziegler *et al.*, *The Stopping and Range of Ions in Solids* (Pergamon, New York, 1985); www.SRIM.org.